

Electronic and Magnetic Properties of a Ferromagnetic Cobalt Surface by Adsorbing Ultrathin Films of Tetracyanoethylene

Stefan Lach,^{1*} Anna Altenhof,^{‡1} Shengwei Shi,^{‡2,3} Mats Fahlman,³ and Christiane Ziegler¹

AUTHOR ADDRESS

- 1) Department of Physics and Research Center OPTIMAS, University of Kaiserslautern, Kaiserslautern, 67663 Kaiserslautern, Germany
- 2) Hubei Key Laboratory of Plasma Chemistry and Advanced materials, School of Materials Science and Engineering, Wuhan Institute of Technology, Wuhan, 430205 Wuhan, China
- 3) Department of Physics, Chemistry and Biology, University of Linköping, Linköping, 58183 Linköping, Sweden

Supporting Information.

Symmetry

When TCNE gets absorbed on the surface, its symmetry is lowered to C_{2v} . This happens for both orientations (face-on bent structure as well as edge-on planar structure), since the mere presence of the surface takes away the one reflection plane (σ_{xy} or σ_{xz} , respectively). The most striking effect is that now the three directions are not equivalent, and thus in the (new) z direction *all* electronic states can lead to optical excitations. Their strength will of course depend on the magnitude of the relevant transition matrix elements. These, in turn, also depend on the fact how strongly the local atomic geometry is distorted (bent structures allow for more excitations due to relaxed selection rules, especially in conjugated systems [s1]). In TCNE the main electronic excitations come from p atomic orbitals, combined into σ , σ^* , π and π^* molecular orbitals. Due to symmetry, the d atomic orbitals will also participate in the π (as well as antibonding π^*) molecular orbitals. The π orbitals belong to the B1u irreducible representation in the free molecule, but to A1 for lying and B2 for standing adsorption. The number of open channels for electronic transitions is the same in both orientations. However, the π orbital in the straight structure still possesses the improper rotation axis \hat{z} even if this is not an element of the point group anymore, thus keeping the numerical values of the relevant integrals, which ultimately count, small. So in the bent structure we expect a higher participation of d -character transitions to the optical excitations.

Adsorption model and coverage estimation:

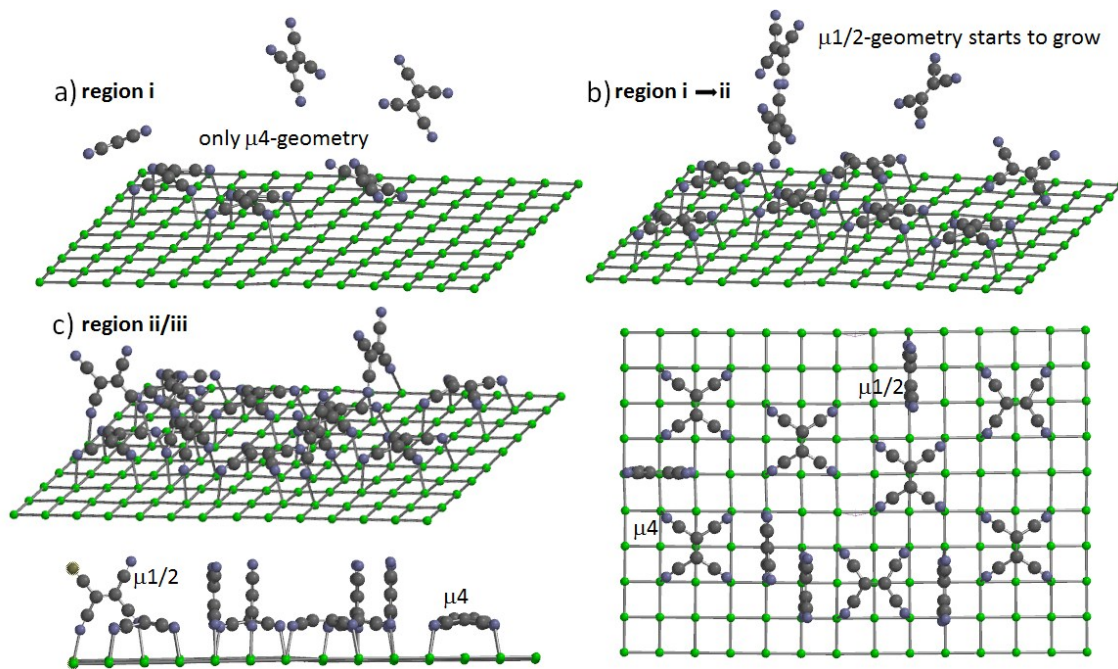


Figure 1s. Extended adsorption model clarifying Fig. 1b in the main article for the three regions i-iii a) for low coverage only face-on adsorption takes place b) transition from pure μ_4 - mixed μ_4 - $\mu_{1/2}$ -adsorption

The discussion of the surface dipole changes for the three coverage regions i-iii shown in fig.1 in the main article, are based on a simple geometric adsorption model also shown in fig.1b and in more details in fig. 1s. To estimate an coverage of TCNE on Co(100), we used the xps core level intensity ratio of the C1s/Co 2 $p_{3/2}$ peaks. We compared the measured TCNE C1s/Co 2 $p_{3/2}$ peak intensity ratio at saturation with that of earlier measurements of the XPS C1s/Co 2 $p_{3/2}$ peak intensities ratio of 1 ML CuPc on Co(100). Here for the face on adsorbed CuPc molecules, a real 1ML coverage was definitively proven by STM. Taking into account, that for the shown surface area above, we only will get 1 CuPc molecule adsorbed [s2], we can estimate the coverage for the TCNE/Co(100) system at saturation coverage $\Theta=1$ to be 3.2×10^{14} molecules/cm².

Further using this C1s/Co 2 $p_{3/2}$ peak reatio method in combination with a simple geometric model for all possible adsorption combinations shown in fig. 2s, we can also estimate the expected coverages for an only μ_4 -, $\mu_{2/1}$ - and mixed μ_4 -/ $\mu_{2/1}$ -geometry. As deducible from the geometries in fig 2s we the get $\Theta_{\mu_4}=1.8 \times 10^{14}$ molecules/cm², $\Theta_{\mu_{2/1}}=5.5 \times 10^{14}$ molecules/cm² and $\Theta_{\mu_4-\mu_{2/1}}=2.5 \times 10^{14}$ molecules/cm² which fits quite well with the experimental found saturation coverage of 3.2×10^{14} molecules/cm².

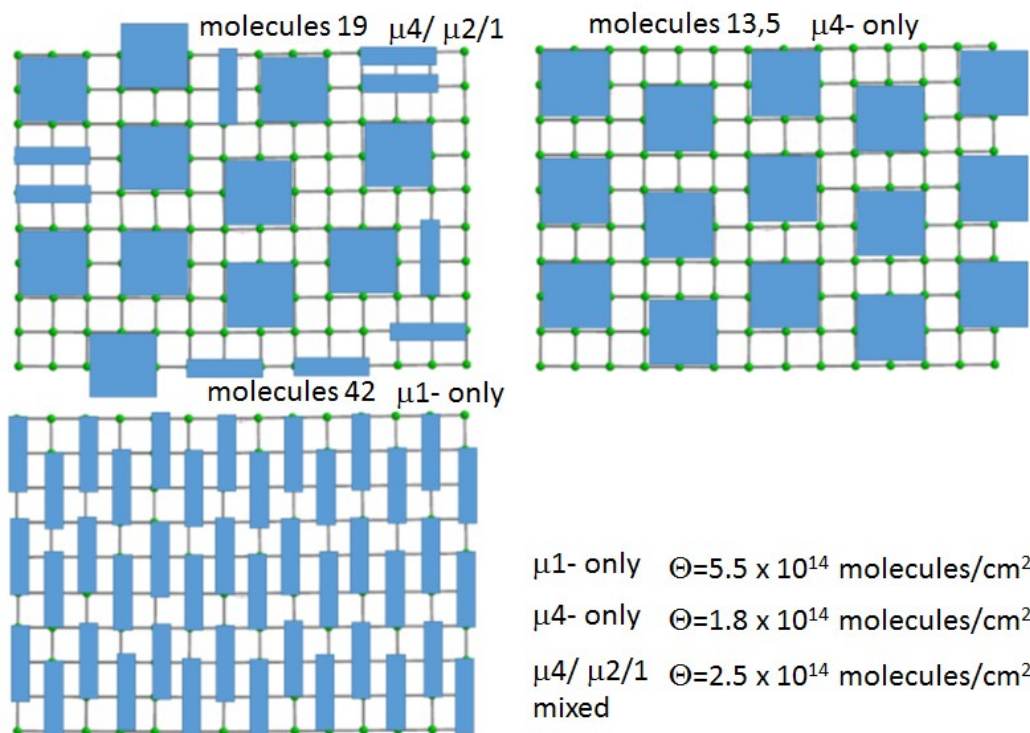


Figure 2s. Possible simple geometric coverage models for the estimation of the saturation coverage in case of pure edge-on or face-on adsorption and the mixed adsorption model we used in this paper.

Equivalent core approximation, z+1 XPS Simulation, Fitting routine:

We simulated XPS-spectra with Koopmans' theorem $-E_b(1s) = \varepsilon(1s)$ and the concept of Hedin and Johansson [s3]. The difference of Hartree-Fock potential of an 1s orbital in the relaxed hole state V^* and the Hartree-Fock potential of the 1s ground state V defining the simple relaxation potential V_R is used to get the binding energy of the 1s-orbital ($E_b(1s)$) by:

$$-E_b(1s) \approx \varepsilon(1s) + \frac{1}{2} \langle 1s | V_R | 1s \rangle \quad \text{eq.1} \quad V_R = \sum_{k=1s} (V^* - V) \quad \text{eq.2}$$

Similar to equation 1 as a simple approach to an interpretation of the relative shifts of the 1s core levels in a relaxed hole state [s4] theoretical calculations using the "equivalent core approximation" or Z+1 approximation were performed [s5] using equation 3.

$$\Delta E_{b,KS}(1s) = \frac{1}{2} [\Delta \varepsilon_{KS} + \Delta \varepsilon_{KS,Z+1}] \quad \text{eq.3}$$

The underlying model assumes a strong localization of core electrons in contrast to only slightly bound valence electrons. The remaining hole, when removing an 1s core electron by photoemission, is simulated by replacing the original nucleus (atomic number Z) by the nucleus of the isoelectronic element with atomic number $Z+1$. The reliability of this model was probed by comparison of measured and calculated 1s binding energies and is reported in several references in literature [s6]. The full calculation of the Kohn Sham energies $\Delta\varepsilon_{KS}/\Delta\varepsilon_{KS,Z+1}$ on the unperturbed D_{2h} geometries of the neutral and anionic states were done using the B3LYP with the 6-31+G*set /6-311G* basis set and Gaussian03/SPARTAN14 software package. Relating the C_{2v} molecular geometry for the bent structure was assumed by the angular information obtained from the NEXAFS data. The equivalent core approximation for C_{2v} was then performed under fixed geometry in single point mode using a 6-31+G*set. For generating a theoretical C1s and N1s spectra, the value of the relative shifts $\Delta E_{b,KS}(1s)$ of the calculated Kohn Sham 1s-energies $\Delta\varepsilon_{KS}/\Delta\varepsilon_{KS,Z+1}$ of the TCNE/anion regarding to the 1s-energies $\Delta\varepsilon_{KS}/\Delta\varepsilon_{KS,Z+1}$ of CH_4 and NH_3 was replaced by a gaussian function of $wG=0.5$ eV.

For both fitting routines on C1s and N1s core level spectra we use PsVoigt2 functions. To estimate the fitting parameter for the PsVoigt2 function we fitted the C1s and the N1s spectra for the pristine TCNE.

Although the C1s signals of the vinyl and the nitrile part cannot be resolved, the fitting of the flank at the lower binding energy side of the pristine TCNE C1s peak can be used to figure out the fitting parameter for the C1s fitting routine used for the adsorbed molecules. Using this parameter also for the pristine TCNE we found a C1s splitting between the vinyl and nitrile C1s signal of 0.5 eV. This value is in the range of spectra using monochromatized X-rays radiation [s7]. The starting peak pattern for the C1s fitting routine on the adsorbed TCNE we get from a theoretical C1s spectrum for a straight and bent TCNE anion (Fig.3 main article). The spectra were generated by folding each calculated Kohn-Sham binding energy from the equivalent core approximation described above, with a gaussian peak function of $wG=0.5$ eV. For the edge-on related peaks (straight= μ_1/μ_2 - geometry) we used a slightly higher $wG=1.7$ eV than for the face-on (bent = μ_4 - geometry) peaks to take into account the more homogeneous C1s shifts in case of a μ_4 adsorption geometry compared to the μ_1/μ_2 -geometry. The N1s structure in Fig. 3s was fitted according to the calculated spectra of the two anion species in Fig. 3sa. By using three instead of only two peaks for the μ_1/μ_2 -geometry we also account for slightly different shifts of the surface attached nitrile-N and the vacuum side nitrile-N. For the condensed layer only straight molecules are expected showing only one N-species. Nevertheless we also calculated the neutral bent/straight spectra showing as expected only a negligible small splitting of 0.08 eV. This shows again the importance of the charge rearrangement in the anionic molecules.

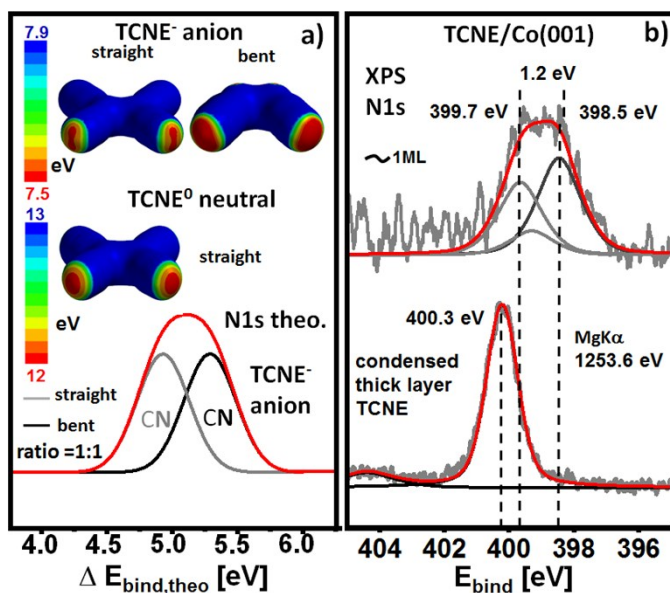


Figure 3s. Peak fitted experimental N1s (c) core level spectra: Comparison of N1s core levels of the system TCNE/Co(100) (upper part, coverage in accordance with coverage region (ii)) with the spectrum of pristine TCNE⁰ found for a thick layer (lower part). (a) lower part: theoretical spectra of the relative core level shifts of the straight (= D2h symmetry) and bent (= C2v symmetry) TCNE anion. Upper part: ionization potential map (bonding, isovalue=0.08) for the neutral and anionic case.

A TCNE²⁻ anion was not considered because it was shown earlier in the literature theoretically and by experiment, that because of the high onsite Coulomb-interaction of 2 eV, the formation of doubly charged TCNE is critical [s8]. Furthermore calculated theoretical NEXAFS spectra at the C K-edge (done in cooperation with Prof. Yi Luo from the KTH) for TCNE²⁻ didn't show any structures around 284 eV which is in contrast to the observed NEXAFS resonances but in line with calculated NEXAFS resonances for TCNE⁻ also showing resonances at 284 eV [s9].

Identification of metal d-contributions using He I and He II.

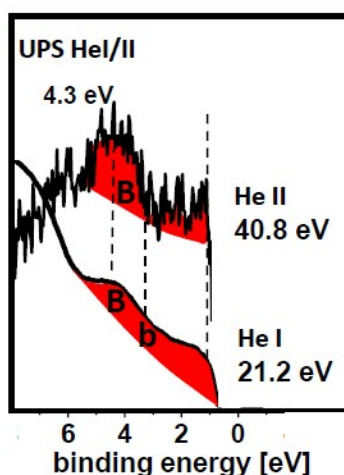


Figure 4s: Comparison of the valence structure of a sub-monolayer in regime (i) measured with He I and He II radiation.

Because of cross section effects the PES intensity of metal atom related d-states increases going from He I=21.2 eV to He II = 40.8 eV and decreases for carbon based p-states [s10]. Therefore in Fig. 4s we can clearly identify valence band state **B** at $E_b=4.3$ eV as a hybrid state with a high metal d band contribution. One can also see that a second structure **b** at $E_b=3.2$ eV has mainly carbon p-state contributions. This will reflect differences in the sp-UPS spectra we found in this region, indicating a spin selective interaction of the metal d-states with the p-states of the TCNE.

TCNE anion DOS by DFT calculation

We performed DFT calculations to simulate the DOS of the two different TCNE anion species. As we did for the simulation of the XPS spectra, in Fig. 5s we simulate the UPS spectra of the single anions by folding of the calculated Kohn-Sham orbitals states with a Gaussian function of $wG=0.5$ eV. The HOMO related structures around -4 eV in Fig. 5s were experimentally and theoretically also found for $RbTCNE_x$ [s8] underlining the cross-section differences we measured in Fig. 4s. The spin density for the single TCNE anion is mainly located at the vinyl side as shown by the spin density map for this anion (Fig5sb). This location of spin at the vinyl side was confirmed for the straight TCNE anion by polarized neutron diffraction [s11].

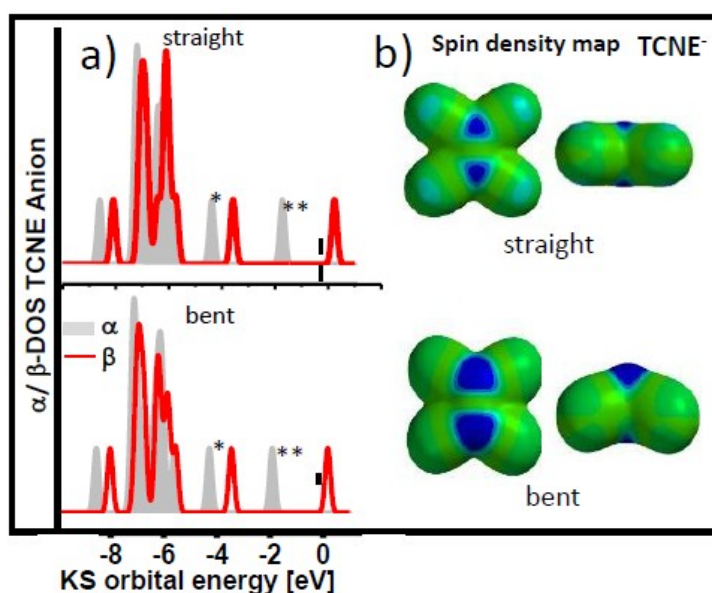


Figure 5s: a) DFT sp-DOS for bent and straight TCNE anions. HOMO/SOMO positions are marked by one/two asterisk. b) Spin density map showing a high localization of the α -spin at the vinyl side.

Model for hardening effect

The tension on the Co surface atoms beneath the TCNE molecule for a μ_4 - adsorption geometry, should cause the edge Co atoms at the nitrile groups of the TCNE to slightly move into the direction of the vinyl group. Concerning the well-known Bethe-Slater curve for cobalt such a reconstruction will lead to an increase of the magnetic exchange coupling constant J between the involved Co atoms. Looking only on one sub unit cell this will not lead to an overall hardening because of the ratio between weaker and stronger interaction is 1/1.

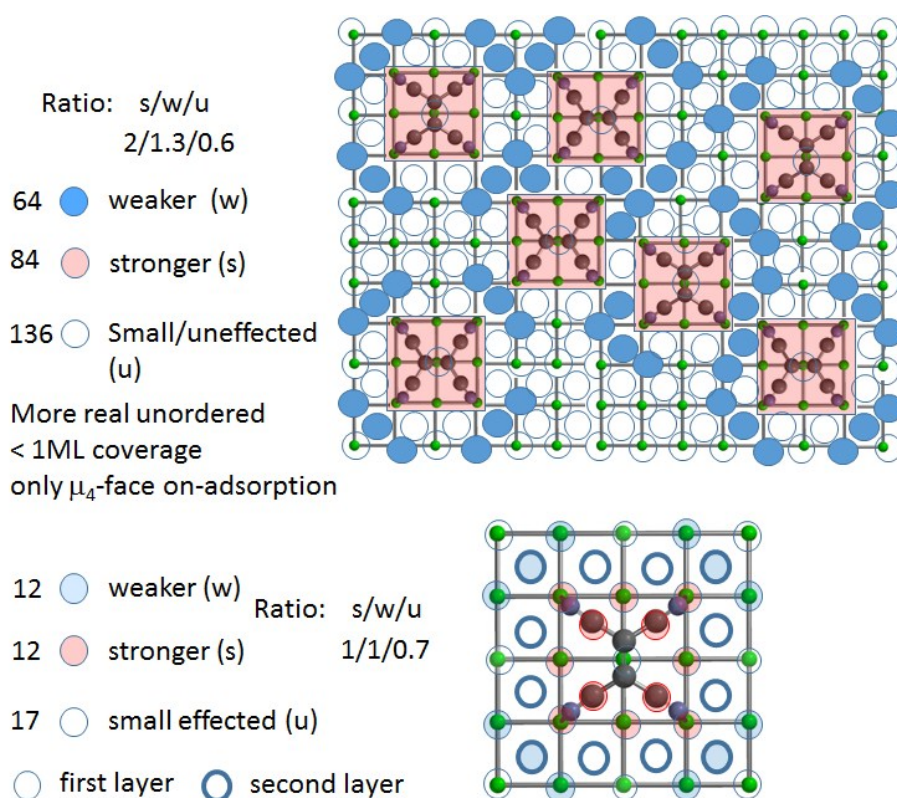


Figure 6s: Tension caused slight compression of the Co structure beneath the adsorbed TCNE. The differences in expected modification in J to the Co atoms and the resulting ratio $n_{\text{stronger}}/n_{\text{weaker}}/n_{\text{small effected}}$ are shown for one sub unit cell and for an ensemble of TCNE molecules adsorbed in a μ_4 -adsorption geometry.

In contrast to TCNE on noble metal surfaces where the molecules are growing in ordered structures [12s-14s], TCNE on a Co(100) surface adsorbs in a hit and stick like reaction with hardly any surface diffusion. This is because of the higher reactivity of the Co surface and well known from our own former experiments on several other organic molecules on Co(100). Therefore, in Fig. 6s, a representative, unordered submonolayer model for adsorption was taken into account. Such an unordered adsorption is supported by LEED. After adsorption of TCNE, the basic (1x1) diffraction pattern of the Co substrate is still visible but the LEED background intensity significantly increases and the 1x1 spots show an enhancement of diffused light, especially visible around (00). Using this simple geometric model it can be shown, that the 1/1 ratio for strengthening and weakening of J (regarding the Bethe-Slater relation for cobalt) for a single TCNE cell will definitively change in favor of a real excess of the stronger J part by a 2/1.3 ratio.

[s1] P. S. Kalsi, *Spectroscopy of organic compounds* (New Age International Publishers, 2005), 6th ed., ISBN 81-224-1543-1.

[s2] S. Lach; A. Altenhof; K. Tarafder; F. Schmitt; M. E. Ali; M. Vogel; J. Sauther; P. M. Oppeneer; C. Ziegler *C. Adv. Funct. Mat.* **2012**, 22, 989

[s3] L. Hedin, G. Johansson, *J. Phys. B*, **2**, 1336 (1969)

[s4] D. Libermann, *Bull. Am. Phys. Soc.* **9**, 731 (1964).

[s5] W. L. Jolly and D. N. Hendrickson, *J. Am. Chem. Soc.* **92**, 1863 (1970).

- [s6] O. Plashkevych, T. Privalov, H. Agren, V. Carravetta, K. Ruud, Chem. Phys. **260**, 11 (2000).
B. Brena, Y. Luo, M. Nyberg, S. Carniato, K. Nilson, Y. Alfredsson, J. Åhlund, N. Mårtensson, H. Siegbahn, C. Puglia, Phys. Rev. B. **70**, 195214 (2004)
J. Wüsten, S. Berger, K. Heimer, S. Lach, Ch. Ziegler J. of Appl. Phys. **98**, 013705/1 (2005)
W. Olovsson, Ch. Göransson, T. Marten, I. A. Abrikosov, phys. stat sol. **243**, 11, 2447 (2006)
T. Yang, B. Dong, J. Wang, Z. Zhang, J. Guan, K. Kuntz, S. C. Warren, David Tomanek, Phys. Rev. B. 125412 (2015)
- [s7] E. Carlegrim, Y. Zhan, F. Li, X. Liu, M. Fahlman, Organic electronics, **11/6**, 1020 (2010)
- [s8] C. Tengstedt, M. Unge, M. P. de Jong, S. Stafstrom, W. R. Salaneck, M. Fahlman Phys. Rev. B **69**, 165208 (2004)
- [s9] Carlegrim, E.; Gao, B.; Kancierzewska, A.; de Jong, M. P.; Wu, Z.; Luo, Y.; Fahlman, M. *Phys. Rev. B* **2008**, 77, 54420
- [s10] Vogel, M.; Schmitt, F.; Sauther, J.; Baumann, B.; Altenhof, A.; Lach, S.; Ziegler, C. *Analyt. Bioanalyt. Chem.*, **400**, 673-678 (2011)
- [s11] A. Zheludev, A. Grand, E. Ressouche, J. Schweizer, B. C. Morin, A. J. Epstein, D. A. Dixon, J. S. Miller, J. Am. Chem. Soc. **116**, 7243 (1994)
- [s12] Wegner, D.; Yamachika, R.; Wang, Y. Brar, V. W.; Bartlett, B. M.; Long, J. R.; Crommie, M. F. Nano Lett. **8**, 131 (2008)
- [s13] Wegner, D.; Yamachika, X. Zhang, R. Wang, Y.; M. F. Crommie, N. Lorente Nano Lett. **13**, 2346 (2013)
- [s14] Bedwani, S.; Wegner, D.; Crommie, M. F.; Rochefort, A. *Phys. Rev. Lett.* **2008**, 101, 216105